

Supporting Information

Dramatically Reducing Critical Velocity of Air Cavity Generation via Biomimetic Microstructure Effect

Zhaochang Wang, Xiaojun Liu, Jiawei Ji, Yunlong Jiao, Kun Liu*

Institute of Tribology, Hefei University of Technology, Hefei 230009, China

KEYWORDS: air-entrained cavity, critical velocity, microstructure effect, moving contact line, drag reduction

* Corresponding author: Jiaoyunlong@hfut.edu.cn

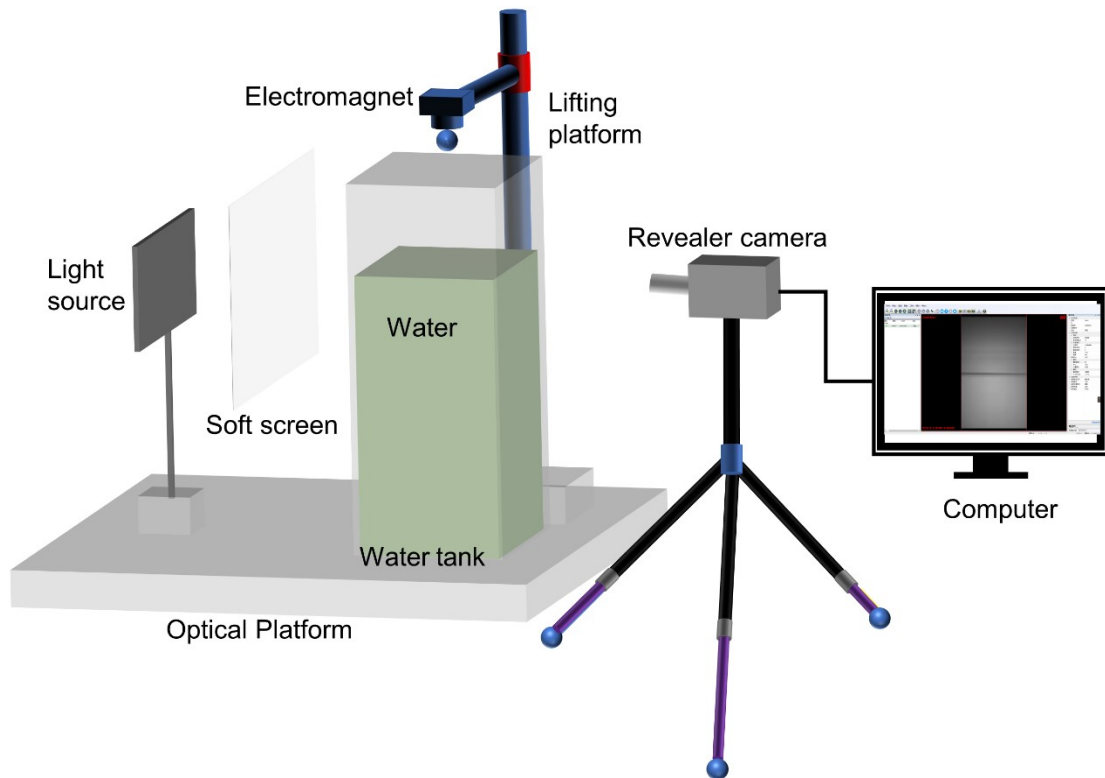


Figure S1. Schematic diagram of experimental device for sphere impacting water surface. The system consists of high-speed video camera (Revealer 5KF10), an electromagnetic system, a 25w surface light source and a PMMA water tank. The sphere is released at any required height by an electromagnetic release system equipped with a lifting platform.

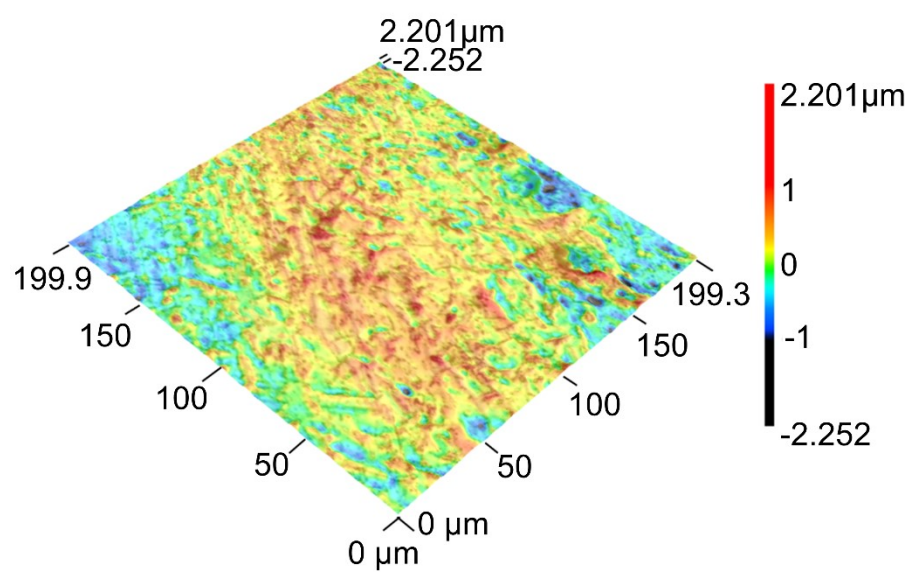


Figure S2. 3D surface morphology of the original sphere

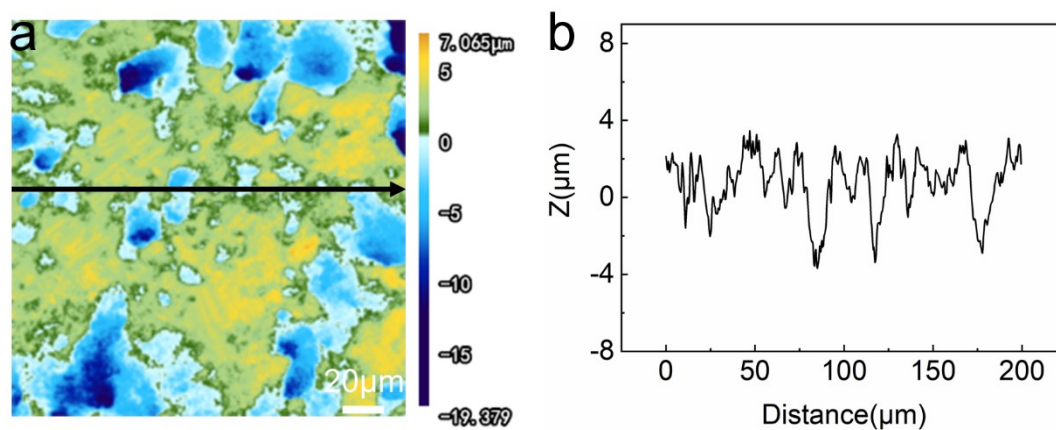


Figure S3. Surface morphology analysis of microstructured spheres by laser confocal microscopy, showing the topography (a) the corresponding skeleton maps (b).

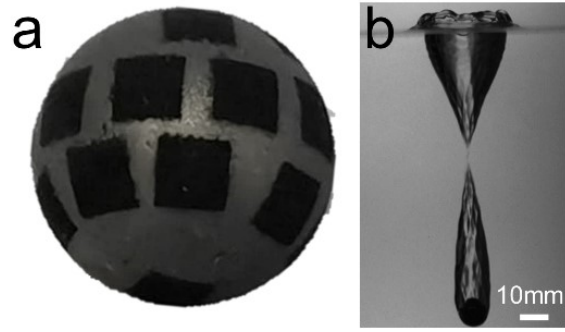


Figure S4. (a) Nanosecond laser-prepared spheres. (b) Water entry of microstructure sphere at an impact velocity of $U = 2.4$ m/s.

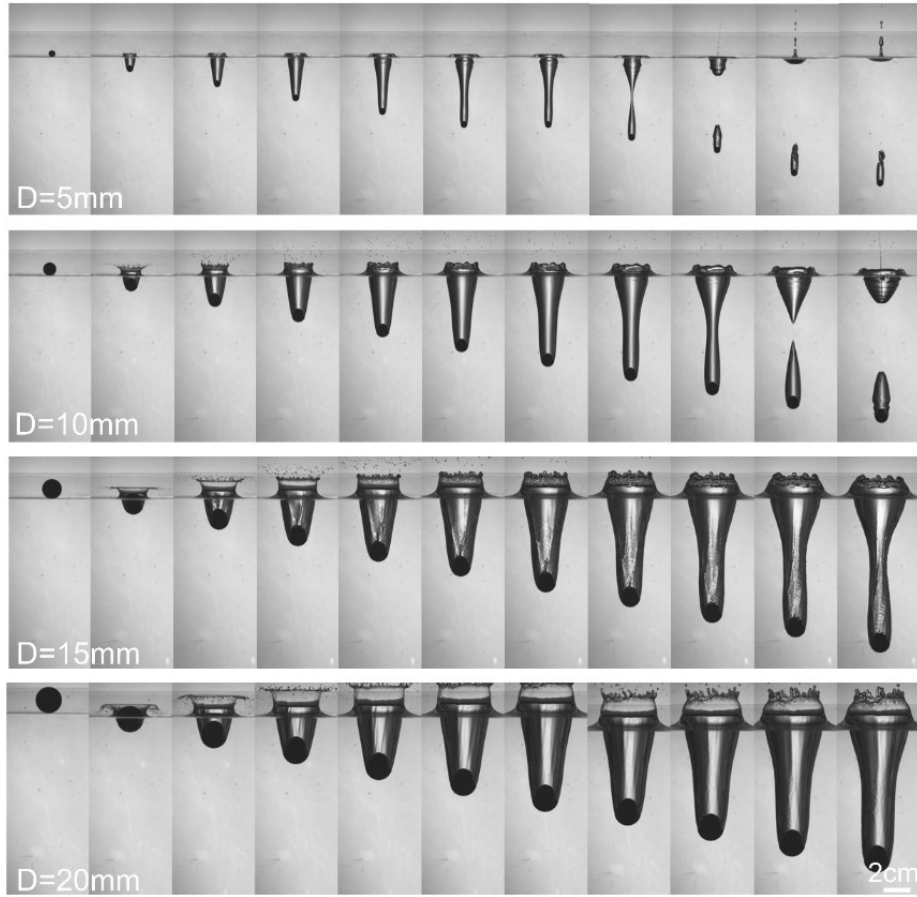


Figure S5. Selected snapshots showing the results of the impact process of microstructured spheres of different diameters ($D=5\text{mm}, 10\text{mm}, 15\text{mm}, 20\text{mm}$) at an impact velocity of $U = 2.4 \text{ m/s}$. The time interval for each image is 5ms.

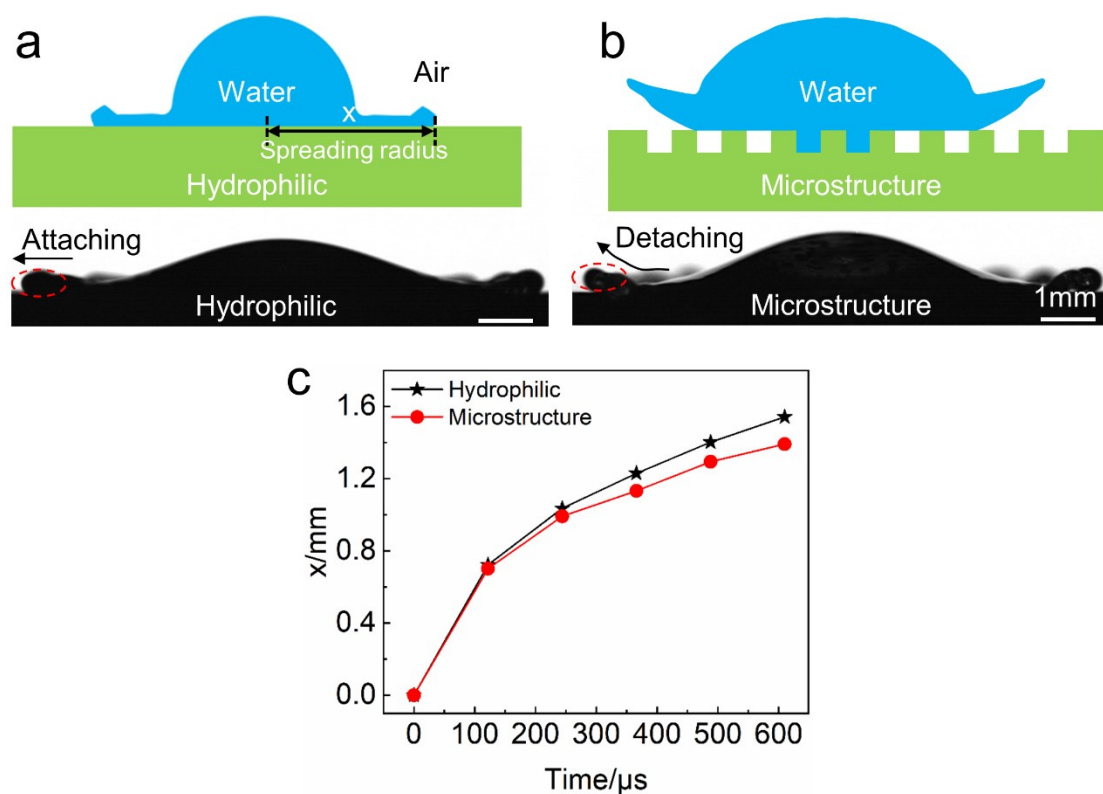


Figure S6. (a and b) The process of liquid film change of deionized water impacting the plane. The liquid film spread along the surface without obvious detachment when droplets impacted the hydrophilic plane. While the liquid film was clearly detached from the surface when the droplets impacted the microstructured plane. (c) Contact line radius as a function of time ($V=18 \mu l$).

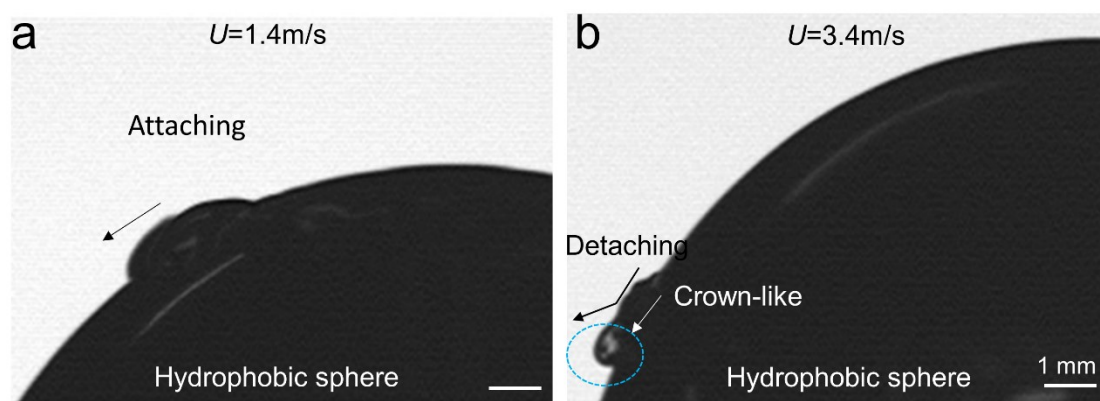


Figure S7. The variation process of liquid film during the deionized water impacting the hydrophobic spheres. (a) The liquid film spread along the surface without obvious detachment when droplets impacted the hydrophobic surface. (b) The liquid film is obviously detached from the surface when the initial impact velocity of the droplet reaches 3.4m/s.

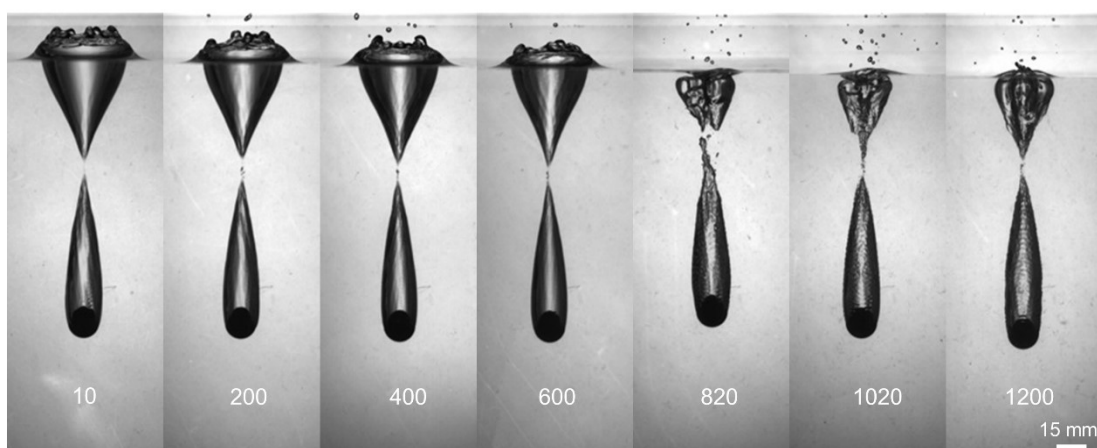


Figure S8. Selected snapshot showed the impacting processes of the microstructured sphere with different times of repetition (10 、200 、400 、600 、820 、1020 and 1200 times). The snapshots were taken just after the cavity pinching off.

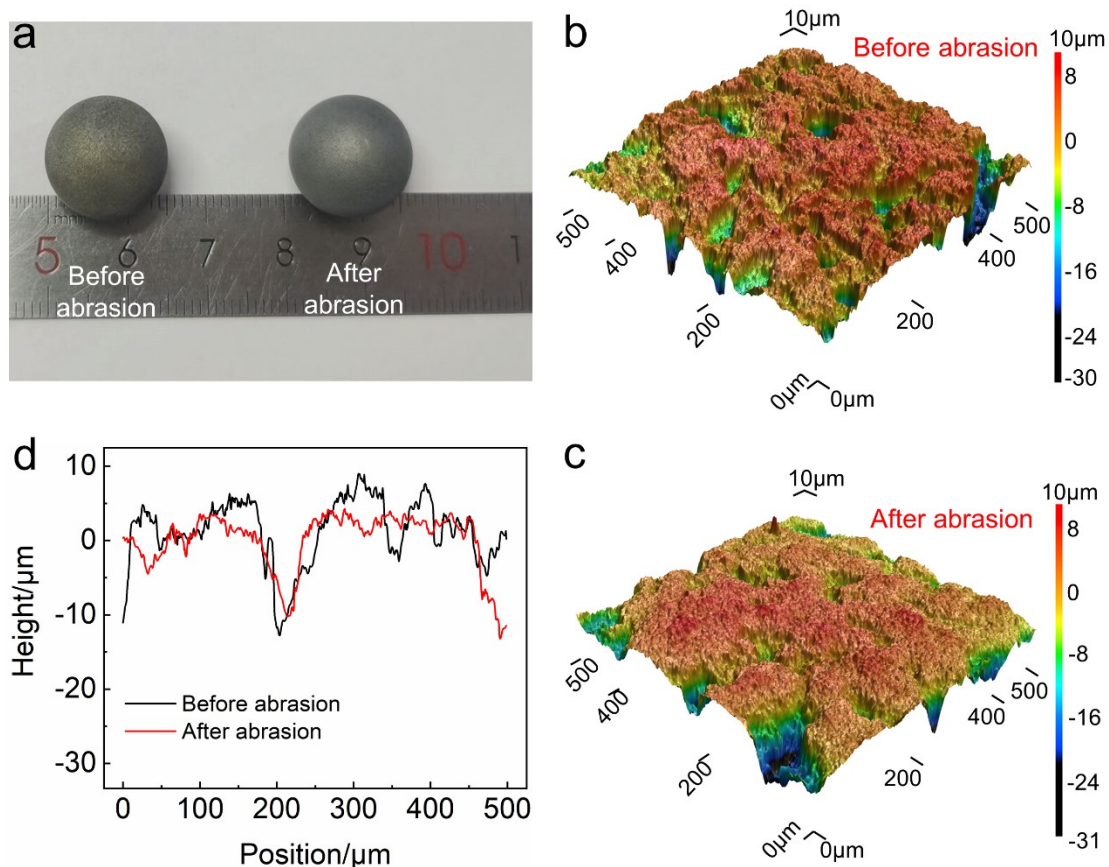


Figure S9. (a) Optical photographs of microstructured spheres ($D=15\text{ mm}$) before and after mechanical abrasion. Surface morphology of microstructured spheres before (b) and after (c) abrasion. (d) Surface height of microstructured spheres before and after abrasion.

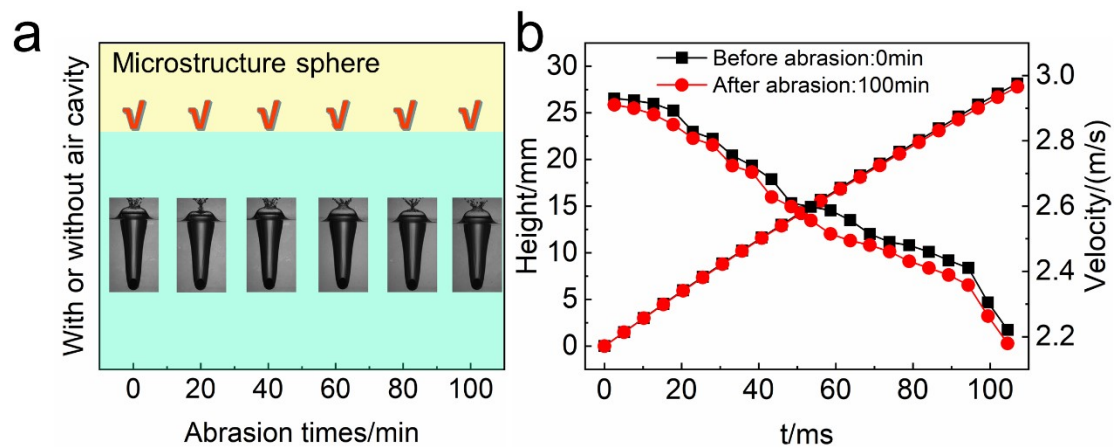


Figure S10. (a) The effect of abrasion time on the sphere into the water air cavity. (b) Kinematic properties of microstructured spheres before and after abrasion.